

MODELING AND ESTIMATION OF MULTI-SOURCE CLUSTERING IN CRIME AND SECURITY DATA¹

BY GEORGE MOHLER

Santa Clara University

While the presence of clustering in crime and security event data is well established, the mechanism(s) by which clustering arises is not fully understood. Both contagion models and history independent correlation models are applied, but not simultaneously. In an attempt to disentangle contagion from other types of correlation, we consider a Hawkes process with background rate driven by a log Gaussian Cox process. Our inference methodology is an efficient Metropolis adjusted Langevin algorithm for filtering of the intensity and estimation of the model parameters. We apply the methodology to property and violent crime data from Chicago, terrorist attack data from Northern Ireland and Israel, and civilian casualty data from Iraq. For each data set we quantify the uncertainty in the levels of contagion vs. history independent correlation.

1. Introduction. Self-exciting point processes have gained attention in recent years for the purpose of modeling criminal activity, in particular, property crime and gang violence [Egesdal et al. (2010), Hegemann, Lewis and Bertozzi (2012), Mohler et al. (2011), Short et al. (2009, 2010), Stomakhin, Short and Bertozzi (2011)], and, more recently, terrorism and other event patterns in extreme security settings [Lewis et al. (2012), Porter and White (2012)]. The defining characteristic of these models is that the occurrence of an event increases the likelihood of more events, as the offender(s) may attempt to replicate a previous success in the same or a nearby location in the following days or weeks [Bowers, Johnson and Pease (2004), Short et al. (2009), Townsley, Johnson and Ratcliffe (2008)]. In Short et al. (2009), a simple procedure is introduced to detect self-excitation in event data, where the distribution of inter-event times $t_i - t_j$ for all $i > j$ is compared to the theoretical distribution corresponding to a stationary Poisson process. For example, we plot in Figure 1 a histogram of the inter-event times $t_i - t_j$ ($i > j$) for civilian casualties per week in Fallujah between March 20, 2003 and December 31, 2007 provided by Iraq Body Count (IBC). The histogram is an estimate of the unnormalized density of inter-event times and is similar to the K -function estimator in Møller and Waagepetersen (2003) [for a uniform distribution on an interval the function decreases linearly, see Short et al. (2009) for further details].

Received August 2012; revised February 2013.

¹Supported in part by ARO Grant 58344-MA and NSF Grant DMS-09-68309.

Key words and phrases. Markov Chain Monte Carlo, Hawkes process, Cox process, crime, terrorism.

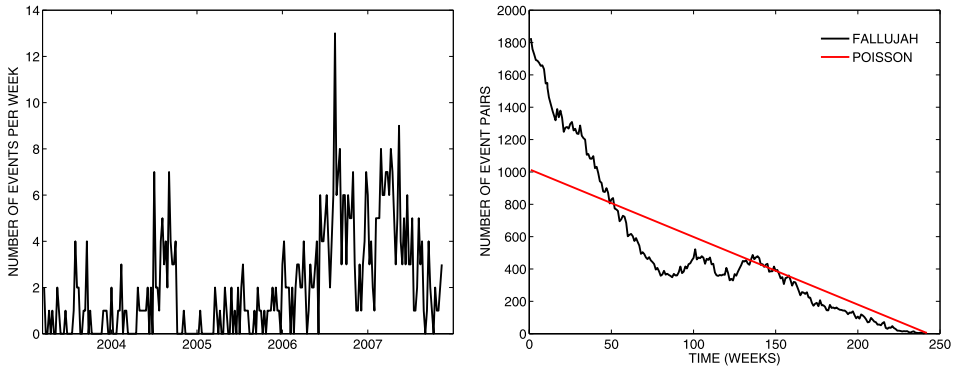


FIG. 1. *Left: Civilian fatalities per week in Fallujah. Right: Distribution of inter-event times.*

The presence of more event pairs at shorter inter-event times compared to random chance provides some evidence that self-excitation may play a role in the occurrence of fatal attacks in Fallujah.

However, other second order point processes are capable of producing clustered inter-event times as depicted in Figure 1. In particular, auto regressive and Cox processes have also been employed as potential models for crime and security related event clustering [Taddy (2010), Zammit-Mangion et al. (2012)]. In these models events are correlated through the intensity of the process, which follows a random trajectory. Whereas for a self-exciting point process the intensity will stay high for a period of time following an event, for a Cox process the intensity may quickly decrease following an event due to random fluctuations. From a social perspective, events may be correlated due to exogenous factors like the state of the economy, month of the year, change in military operations, etc., rather than “caused” by endogenous factors such as repeat offender behavior.

We propose a model along with an efficient inference methodology for quantifying uncertainty in the levels of contagion vs. history independent correlation in crime and security data sets. The model consists of a discrete time Hawkes process with background rate determined by a log Gaussian Cox process (LGCP). The Gaussian process is given by the forward Euler discretization of a mean reverting Ornstein–Uhlenbeck stochastic differential equation. Details of the model are provided in Section 2. For filtering of the intensity and estimation of the model parameters, we consider an extension of the Metropolis adjusted Langevin algorithm (MALA) for LGCPs to the case of self-excitation. By exploiting properties of the covariance matrix of the model in Section 2, MALA can be implemented such that the cost of each metropolis iteration scales linearly with the size of the data. Details of the inference methodology are provided in Section 3. In Section 4 we validate the methodology on synthetic data and then apply it to several open source crime and security data sets: property and violent crime in Chicago, terrorist attacks in Northern Ireland and Israel, and civilian casualties in Fallujah, Iraq.

We confirm previous work suggesting that contagion plays a role in crime event clustering, though our results indicate that correlated fluctuations are also important. For data sets corresponding to more extreme security settings, we observe a wider range in the levels of contagion.

2. A Hawkes–Cox process model of crime and security. We consider a discrete time model for the intensity of events where the background rate is determined by a Log Gaussian Cox process (LGCP) and the intensity is self-excited by the occurrence of events. In particular, the intensity is given by

$$(1) \quad \lambda_i = e^{x_i} + \sum_{i>j} \theta \frac{(1-b)}{b} b^{i-j} y_j,$$

where y_i is the number of events and λ_i is the expected number of events in the time interval $[i \Delta t, (i + 1) \Delta t]$. The parameters θ and b control the level and timescale of contagion effects and we use the initial conditions $\lambda_0 = e^\mu$ throughout. Here x_i is a Gaussian process with mean μ and covariance matrix Σ , where

$$(2) \quad \Sigma_{ij} = \sigma^2 a^{|i-j|}.$$

The model is capable of producing event clustering due to both contagion effects and history independent correlations. For example, $\theta = 0$ corresponds to a LGCP and $\sigma^2 = 0$ corresponds to a discrete time version of a Hawkes process. The parameters a and b control the timescales over which history independent correlation and contagion effects persist. In Figure 2 we plot two realizations of the intensity (1), one corresponding to a LGCP without self-excitation and one corresponding to a Hawkes process with constant background rate. We note that in both cases significant clustering is observed and it is difficult to distinguish the type of clustering based upon visual inspection of the intensity. We will return to this example in Section 4.

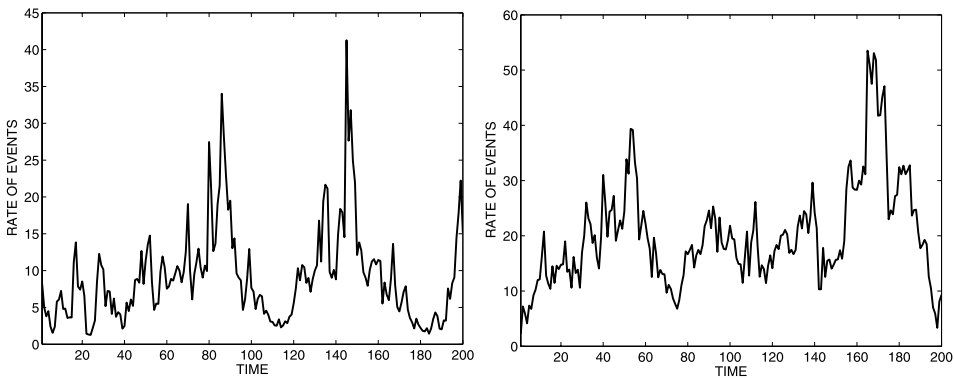


FIG. 2. Left: Cox process with parameters $a = 0.9$, $\sigma^2 = 0.7$ and $\mu = 1.8$. Right: Hawkes process with parameters $\mu = 0.8$, $b = 0.075$ and $\theta = 0.9$.

The model given by equation (1) is related to the standard continuous time Hawkes process,

$$(3) \quad \lambda(t) = \nu + \sum_{t > t_i} k(t - t_i),$$

where λ is the intensity (rate) of events, ν is the background (Poisson) rate of events, and $k(t - t_i)$ is a triggering kernel that determines the distribution of offspring events generated by events t_i from the history of the process. Hawkes processes are used to model risk increases triggered by events in the history of the process and have been applied to repeat offender behavior in burglary [Mohler et al. (2011)], retaliations in gang violence [Egesdal et al. (2010), Hegemann, Lewis and Bertozzi (2012), Short et al. (2010), Stomakhin, Short and Bertozzi (2011)] and terrorist and insurgent activity [Lewis and Mohler (2011), Porter and White (2012)]. Continuous time Log Gaussian Cox processes are also used to model event clustering, for example, in Brix and Diggle (2001) a mean reverting Ornstein–Uhlenbeck SDE is used to determine the intensity of the point process. For an exponential kernel (3) can be written as a differential equation and a continuous time Hawkes–Cox process is governed by the system of stochastic differential equations,

$$(4) \quad dx_t = -\omega_1(x_t - \mu) dt + \alpha_1 dB_t,$$

$$(5) \quad dg_t = -\omega_2 g_t dt + \alpha_2 \omega_2 dN_t, k,$$

where B_t is a standard Brownian motion and N_t is a point process with conditional intensity

$$(6) \quad \lambda_t = e^{x_t} + g_t.$$

Here the parameters ω_1 and ω_2 determine the timescale over which clustering due to history independent correlations and contagion last, α_1 and α_2 determine the size of intensity fluctuations, and μ determines the baseline level of event activity.

To facilitate simulation and estimation, in addition to the fact that many crime and security data sets are binned by day or some other time unit, we restrict our attention to discrete forward Euler approximations,

$$(7) \quad x_i = x_{i-1} - \omega_1(x_{i-1} - \mu)\Delta t + \alpha_1 \sqrt{\Delta t} Z_{i-1},$$

$$(8) \quad g_i = g_{i-1} - \omega_2 g_{i-1} \Delta t + \alpha_2 \omega_2 y_{i-1},$$

where $Z_{i-1} = \mathcal{N}(0, 1)$ and y_{i-1} is the number of events occurring in $[(i - 1)\Delta t, i\Delta t]$. Letting $a = (1 - \omega_1 \Delta t)$, $\sigma^2 = \alpha_1^2 \Delta t / (1 - (1 - \omega_1 \Delta t)^2)$, $b = (1 - \omega_2 \Delta t)$ and $\theta(1 - b) = \alpha_2 \omega_2$, the discrete model takes the form of (1).

3. Filtering and estimation using MALA. In this section we discuss general strategies for point process estimation and then develop an inference methodology for simultaneously filtering the latent Gaussian process x_i and estimating the parameters $(a, \sigma^2, \mu, b, \theta)$ from observations y_i assumed to have been generated by

a model of the form (1). Our goal will be to quantify the uncertainty in the level of contagion present in an event time series, as well as to detect history independent correlation that may also be present. In particular, we will use Markov Chain Monte Carlo to obtain a posterior probability distribution for the intensity of the process, the latent Gaussian process and the model parameters.

For Hawkes processes with stationary background rate, EM-type algorithms are a popular choice and parametric and variational versions are used in seismological and security related applications [Lewis and Mohler (2011), Marsan and Lengliné (2008), Mohler et al. (2011), Sornette and Utkin (2009), Veen and Schoenberg (2008)]. One issue that arises, however, is that parameter estimates suffer from high variance when the clusters are not well separated [Lewis and Mohler (2011), Sornette and Utkin (2009)], a common problem for the EM algorithm applied to mixture models (the Hawkes process in equation 3 can be viewed as a mixture model with the number of mixtures equal to the number of points in the data set). With the introduction of a nonstationary LGCP background rate, EM estimates are likely to have even higher variation. We will therefore take a Bayesian approach to the estimation problem in order to quantify the uncertainty in parameter estimates.

We note that a variety of methods have been developed for the estimation of temporal point processes, including EM algorithms [Smith and Brown (2003)], variational alternatives [Mangion et al. (2011)], integrated nested Laplace approximations [Rue, Martino and Chopin (2009)] and expectation propagation [Cseke and Heskes (2011)]. As discussed in Brix and Diggle (2001), sequential filtering for LGCPs suffers from large variance of the importance weights and the authors instead use the Metropolis adjusted Langevin algorithm (MALA) for filtering the intensity of LGCPs after estimating the parameters via a moment-based method. Similar jump diffusion models to (4)–(5) have recently been used to model financial contagion. In Giesecke and Schwenkler (2011), an approximate likelihood filter is employed that avoids the need for Monte Carlo simulation, though the computational cost of the method prevents the straightforward extension to spatial processes. For simultaneous filtering of the intensity and estimation of parameters, Langevin and Hamiltonian Monte Carlo methods on manifolds are developed in Girolami and Calderhead (2011) capable of handling high-dimensional/spatial problems. We take this approach as well, though we avoid the need for manifold based Monte Carlo by exploiting an analytic expression for the inverse covariance matrix of the process.

3.1. *Metropolis adjusted Langevin algorithm.* In general, given a random vector $\vec{\theta}$ with density $\pi(\vec{\theta})$, the stochastic differential equation (Langevin equation),

$$(9) \quad d\vec{\theta}(t) = \nabla_{\vec{\theta}} \log(\pi(\vec{\theta})) dt/2 + dB(t),$$

has stationary distribution $\pi(\vec{\theta})$. The forward Euler discretization of (9) is given by

$$(10) \quad \vec{\theta}^* = \vec{\theta}^n + \frac{\varepsilon^2}{2} \nabla_{\vec{\theta}} \log(\pi(\vec{\theta}^n)) + \varepsilon Z_n,$$

which no longer has the correct stationary distribution, nor satisfies detailed balance. These shortfalls are overcome through MALA by adjusting the Langevin equation with a Metropolis acceptance condition after each Euler step. The transition density is given by

$$(11) \quad q(\vec{\theta}^*|\vec{\theta}^n) = \mathcal{N}\left(\vec{\theta}^n + \frac{\varepsilon^2}{2} \nabla_{\vec{\theta}} \log(\pi(\vec{\theta}^n)), \varepsilon^2 I\right)$$

and the acceptance probability is

$$(12) \quad \min\left\{1, \frac{q(\vec{\theta}^n|\vec{\theta}^*)\pi(\vec{\theta}^*)}{q(\vec{\theta}^*|\vec{\theta}^n)\pi(\vec{\theta}^n)}\right\}.$$

The posterior density for the discrete Hawkes–Cox process is given by

$$(13) \quad \begin{aligned} &\pi(\vec{x}, a, \sigma^2, \mu, b, \theta|\vec{y}) \\ &\propto \left(\prod_{i=1}^N \exp\{-\lambda_i\} \lambda_i^{y_i}\right) |\Sigma|^{-1/2} \exp\{-(\vec{x} - \mu 1)^T \Sigma^{-1} (\vec{x} - \mu 1)/2\} \\ &\quad \times p(a, \sigma^2, \mu, b, \theta), \end{aligned}$$

where $p(a, \sigma^2, \mu, b, \theta)$ is the prior distribution of the model parameters. The derivatives of the posterior density are given by

$$(14) \quad \nabla_{\vec{x}} \log(\pi) = \vec{v} - \Sigma^{-1}(\vec{x} - \mu 1),$$

where $v_i = y_i \exp\{x_i\}/\lambda_i - \exp\{x_i\}$,

$$(15) \quad \begin{aligned} \nabla_a \log(\pi) &= -0.5 \frac{d \log(|\Sigma|)}{da} + 0.5(\vec{x} - \mu 1)^T \Sigma^{-1} \frac{d\Sigma}{da} \Sigma^{-1}(\vec{x} - \mu 1) \\ &\quad + \frac{d \log(p)}{da}, \end{aligned}$$

$$(16) \quad \begin{aligned} \nabla_{\sigma^2} \log(\pi) &= -0.5 \frac{d \log(|\Sigma|)}{d\sigma^2} + 0.5(\vec{x} - \mu 1)^T \Sigma^{-1} \frac{d\Sigma}{d\sigma^2} \Sigma^{-1}(\vec{x} - \mu 1) \\ &\quad + \frac{d \log(p)}{d\sigma^2}, \end{aligned}$$

$$(17) \quad \nabla_{\mu} \log(\pi) = \sum_{i=1}^N (\Sigma^{-1}(\vec{x} - \mu 1))_i + \frac{d \log(p)}{d\mu},$$

$$(18) \quad \nabla_b \log(\pi) = \sum_{i=1}^N (y_i/\lambda_i - 1) \frac{d\lambda_i}{db} + \frac{d \log(p)}{db}$$

and

$$(19) \quad \nabla_{\theta} \log(\pi) = \sum_{i=1}^N (y_i/\lambda_i - 1) \frac{d\lambda_i}{d\theta} + \frac{d \log(p)}{d\theta}.$$

In general, each Metropolis proposal is associated with $O(N^3)$ operations, as the inverse covariance matrix and the determinant are required. However, these can be determined analytically for our covariance matrix [Shaman (1969)]:

$$(20) \quad \Sigma^{-1} = \frac{1}{\sigma^2(1-a^2)} \begin{bmatrix} 1 & -a & 0 & \dots & 0 \\ -a & 1+a^2 & -a & \dots & 0 \\ 0 & \ddots & \ddots & \ddots & 0 \\ \vdots & & & -a & 1+a^2 & -a \\ 0 & \dots & 0 & -a & 1 & 1 \end{bmatrix}$$

and

$$(21) \quad |\Sigma| = \sigma^{2N} (1-a^2)^{N-1}.$$

Because Σ^{-1} is tridiagonal, (13) and (14) require $O(N)$ operations to evaluate. Furthermore, the derivatives on the right side of (15) and (16) can be computed directly from (13), (20) and (21). The recursive relationship,

$$(22) \quad \lambda_i - e^{x_i} = b(\lambda_{i-1} - e^{x_{i-1}}) + \theta(1-b)y_{i-1},$$

can be used to compute λ_i , $\frac{d\lambda_i}{db}$ and $\frac{d\lambda_i}{d\theta}$ efficiently in $O(N)$ operations.

4. Results. In this section we validate the inference methodology of Section 3 on synthetic data generated by the discrete Hawkes–Cox process model introduced in Section 2. We then apply the methodology to several open source crime and terrorism data sets to estimate the levels of contagion and history independent correlation present in the data.

For all examples we use the following MCMC iteration procedure. At each iteration we alternately sample first the latent variable, \vec{x} , using equations (11)–(12) with Langevin step size $\varepsilon = 0.1$, second the variables a , σ^2 and μ with step size $\varepsilon = 0.01$, and third the parameters b and θ with step size $\varepsilon = 0.01$. We note that the second and third steps are independent, as the parameters are only coupled through their dependence on \vec{x} . We use $U[0, 1]$ priors for the parameters a , b and θ , and $\mathcal{N}(0, 5)$ priors for μ and σ^2 (σ^2 restricted to be positive). $5 \cdot 10^5$ Monte Carlo iterations are used in each example with a burn-in of $2.5 \cdot 10^5$. Trace plots of the posterior distribution are inspected to verify convergence.

4.1. *Example 1: Two sources of correlation.* We first validate the inference methodology for a discrete Hawkes–Cox process with $N = 500$ time steps and parameters $a = 0.65$, $\sigma^2 = 1$, $\mu = 2$, $b = 0.35$, and $\theta = 0.5$. Convergence to the stationary distribution is reached in less than 10^5 MCMC iterations, as illustrated by the trace plots of the posterior parameter distributions shown in Figure 3. For an arbitrary covariance matrix the cost of one Monte Carlo step would be $O(500^3)$, but due to the linear dependence on the size of the data, we were able to take

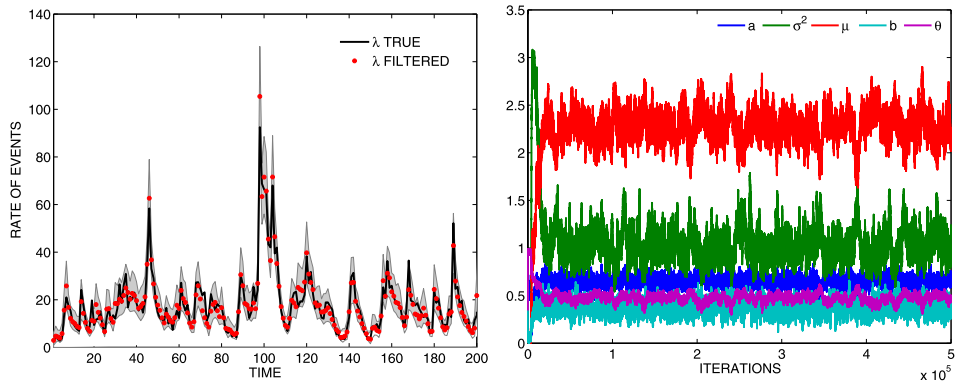


FIG. 3. *Left: First 200 time units of the simulated intensity (black) along with the filtered intensity (posterior mean in red, 95% range in grey) with $N = 500$, $a = 0.65$, $\sigma^2 = 1$, $\mu = 2$, $b = 0.35$, and $\theta = 0.5$. Right: Trace plots of the posterior parameter distributions.*

$5 \cdot 10^5$ Monte Carlo steps implemented in Matlab with a 1.8 GHz dual-core Intel i7 processor in less than 2 hours.

We confirm the accuracy of the methodology by plotting the filtered intensity (posterior mean) against the true intensity of the simulated Hawkes–Cox process (first 200 time units for visualization) in Figure 3. The shaded region indicates the 95% range of the posterior intensity. In Figure 4 we plot the posterior distribution of the five model parameters along with the true parameters (indicated by a red vertical line) used in the simulation. The relative error between the true parameter value and the posterior mean is less than 14% for all parameters. We note that for a particular realization of the point process the posterior distribution for the estimate of μ appears biased, however, for different realizations of the intensity the estimate may over- or underestimate μ .

4.2. Example 2: Contagion vs. history independent correlation. We return to the example plotted in Figure 2 in order to assess whether the Langevin Monte Carlo method can distinguish between a Hawkes process and a Cox process.

For the Cox process we use the parameters $a = 0.9$, $\sigma^2 = 0.7$ and $\mu = 1.8$ ($\theta = 0$) with $N = 200$. The Hawkes portion of the intensity $\lambda - e^x$ thus equals zero in equation (1). In Figure 5 (left) we plot the true intensity of the simulated Cox process (black) along with the filtered intensity (posterior mean in red) and the filtered Hawkes portion of the intensity (posterior mean in blue). We note that the Hawkes portion of the estimated intensity remains close to zero throughout the time interval, though for periods of high event activity it accounts for up to 1/6 of the overall rate of events. Thus, one needs to be cautious in interpreting results for similar levels of contagion inferred from crime and security data sets.

For the Hawkes process with constant background rate we use the parameters $\mu = 0.8$, $b = 0.075$ and $\theta = 0.9$ ($\sigma = 0$) with $N = 200$. In Figure 5 (right) we plot the true intensity λ (black) and background rate e^x (dashed black) against the

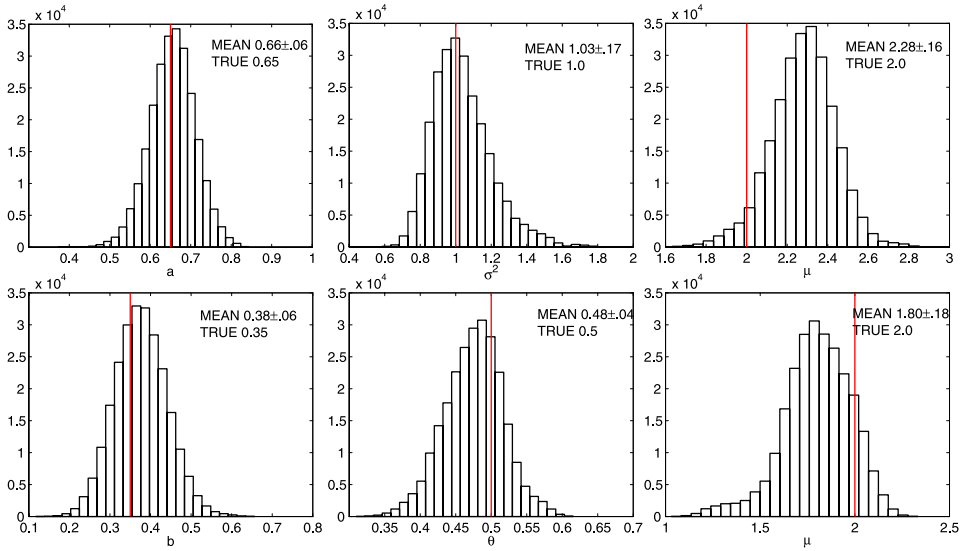


FIG. 4. Histograms of the sampled posterior parameter distributions (250,000 samples) corresponding to a simulated point process with parameters $a = 0.65$, $\sigma^2 = 1$, $\mu = 2$, $b = 0.35$, and $\theta = 0.5$. The posterior mean and standard deviation are displayed in the top right of each figure and the red line indicates the true value of the parameter used to simulate the intensity. The lower right posterior distribution for the parameter μ corresponds to a different realization of the point process.

filtered intensity (posterior mean in red) and Cox contribution to the estimated intensity (blue dots). We note that the filtered background rate exhibits low variation and provides a good approximation to the actual background rate, $\exp(0.8)$.

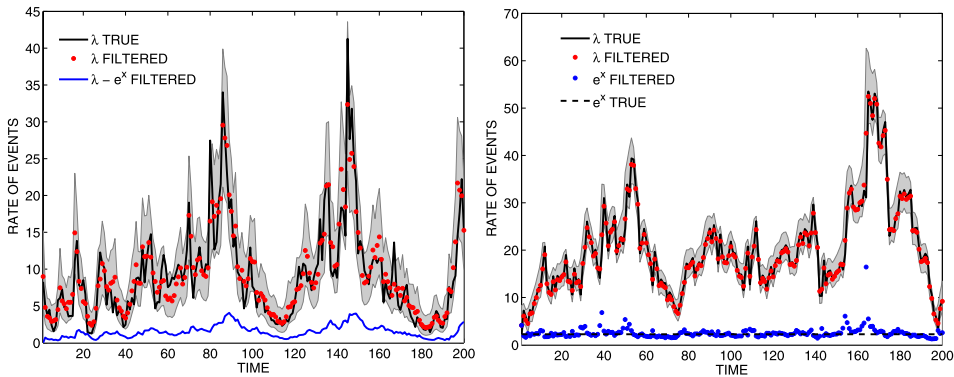


FIG. 5. Left: Simulated intensity (black) of a Cox process with parameters $a = 0.9$, $\sigma^2 = 0.7$ and $\mu = 1.8$ along with the filtered intensity (posterior mean in red, 95% range in grey, and estimated Hawkes portion of the intensity in blue). Right: Simulated intensity (black) of a Hawkes process with parameters $\mu = 0.8$, $b = 0.075$ and $\theta = 0.9$ along with the filtered intensity (posterior mean in red, 95% range in grey, and estimated Cox portion of the intensity in blue).

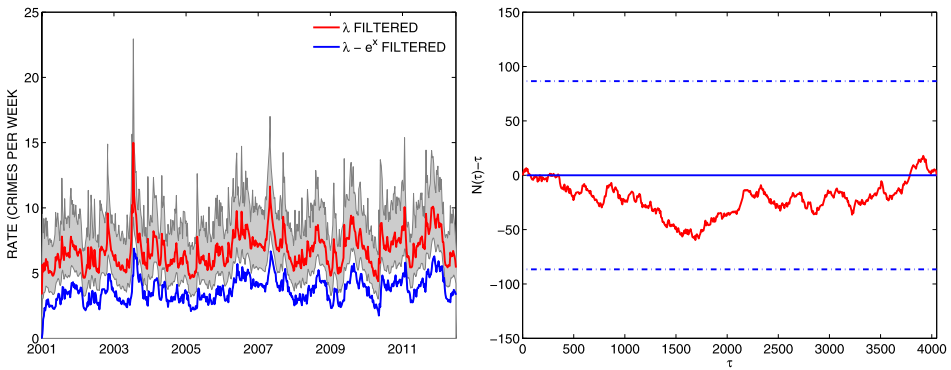


FIG. 6. Property crime in Chicago. Left: Filtered intensity λ (posterior mean in red, 95% range in grey) and Hawkes rate $\lambda - e^x$ (posterior mean in blue). Right: Normalized cumulative distribution of rescaled event times along with 95% error bounds of the Kolmogorov–Smirnov statistic.

4.3. *Application to crime and security data.* Next we apply the inference methodology to several open source crime and security data sets to assess the sources of clustering. The first data set is the counts per week of property crime (burglary and motor vehicle theft) and violent crime (battery, assault and robbery) occurring in Beat 423 in Chicago between January 1, 2001 and June 15, 2012. The data is available through the Chicago data portal at <https://data.cityofchicago.org/Public-Safety/Crimes-2001-to-present/ijzp-q8t2>. The terrorism data sets we use include the counts per week of attacks in Israel (2001–2010) and Northern Ireland (1970–1993). The data is available through the Global Terrorism Database at <http://www.start.umd.edu/gtd/>. The civilian casualty data from Fallujah described in Section 1 can be obtained through the IBC at <http://www.iraqbodycount.org/database/>.

In Figure 6 we plot the filtered intensity for property crime in Chicago and in Figure 7 we plot the filtered intensity for violent crime. In order to assess the goodness of fit of the model, we use residual analysis [Ogata (1988)]; the rescaled event times

$$(23) \quad \tau_i = \int_0^{t_i} \lambda(t) dt$$

are distributed according to a unit rate Poisson process if the model is correctly specified. On the right of Figures 6 and 7 we plot the normalized cumulative number of events $N(\tau) - \tau$ against the rescaled event times τ .

For property crime 45% of the events are attributed to the background rate e^x and the other 55% are attributed to the Hawkes component (see Table 1). The posterior standard deviation for the percentage of events assigned to the Hawkes intensity is 7%, thus indicating with a high degree of certainty that both types of correlation are playing a significant role in intensity fluctuations. The time scale

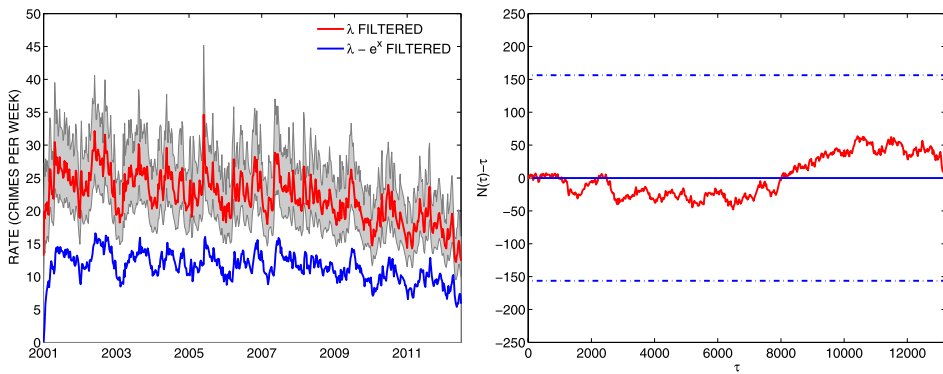


FIG. 7. Violent crime in Chicago. Left: Filtered intensity λ (posterior mean in red, 95% range in grey) and Hawkes rate $\lambda_i - e^{x_i+c-i}$ (posterior mean in blue). Right: Normalized cumulative distribution of rescaled event times along with 95% error bounds of the Kolmogorov–Smirnov statistic.

parameter ω_1^{-1} of mean reversion of the Cox process is estimated to be 1.7 weeks and for the Hawkes triggering kernel the time scale ω_2^{-1} is estimated to be 4.8 weeks. A number of exogenous factors fluctuating on a weekly basis could be causing the correlated fluctuations, such as weather or routine activities linked to work and pay schedules. The several week duration of self-excitation is consistent with previous estimates for property crime. We also note that the normalized cumulative distribution of rescaled event times stays well within the 95% error bounds of the Kolmogorov–Smirnov statistic.

The Chicago violent crime data and the Northern Ireland terrorist attack data both exhibit significant slow timescale trends over the observation window. To account for this in the model, we multiply the background rate e^{x_i} by an exponential factor $e^{c \cdot i}$ and estimate c along with the other model parameters using MALA. For violent crime we observe similar levels of contagion and correlation, as well as similar timescales to the property crime time series. With the addition of the exponential factor in the model, $N(\tau) - \tau$ stays well within the 95% error bounds.

TABLE 1

Posterior mean and standard deviation of the percentage of events attributed to the Hawkes component of the estimated intensity (top row) and posterior mean of the timescales ω_1^{-1} and ω_2^{-1} in weeks associated with the Cox and Hawkes processes, respectively (bottom two rows)

	Prop.	Viol.	N. Ireland	Israel	Fallujah
% Hawkes	55 (7)	52 (7)	50 (5)	12 (7)	23 (13)
Timescale Cox	1.7	1.5	1.7	2.8	36.0
Timescale Hawkes	4.8	3.9	9.3	5.7	4.9

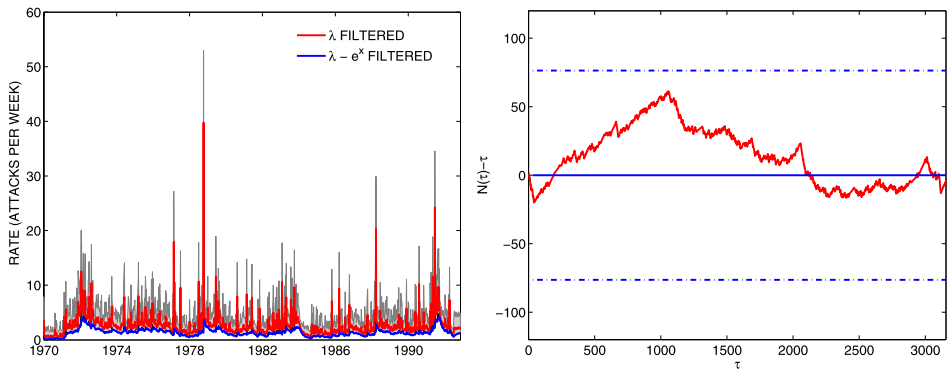


FIG. 8. *Terrorist attacks in Northern Ireland. Left: Filtered intensity λ (posterior mean in red, 95% range in grey) and Hawkes rate $\lambda_i - e^{x_i+c-i}$ (posterior mean in blue). Right: Normalized cumulative distribution of rescaled event times along with 95% error bounds of the Kolmogorov–Smirnov statistic.*

In Figure 8 we plot the filtered intensity for terrorist attacks in Northern Ireland. The estimated dynamics of the process have similarities to the Chicago crime data set, as the percentage of events attributed to contagion is $50\% \pm 5\%$. The timescale over which the estimated self-excitation lasts, 9.3 weeks, is the longest out of all of the data sets explored here. In contrast, we plot the corresponding intensities for terrorist attacks in Israel in Figure 9 and for civilian casualties in Figure 10. In Israel, we observe very little contagion effects, similar to those in Figure 5. The timescale associated with history independent correlation in Iraq is the slowest out of all 5 data sets, at 36 weeks. This is likely due to exogenous factors such as troop surges playing a large role in intensity fluctuations. However, a significant

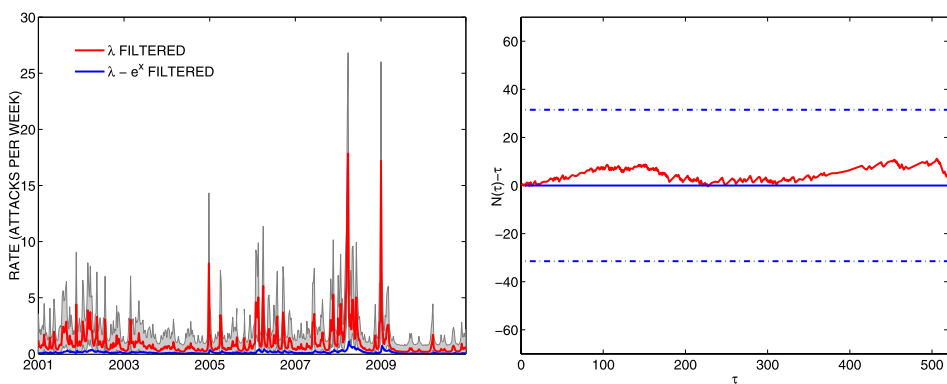


FIG. 9. *Terrorist attacks in Israel. Left: Filtered intensity λ (posterior mean in red, 95% range in grey) and Hawkes rate $\lambda - e^x$ (posterior mean in blue). Right: Normalized cumulative distribution of rescaled event times along with 95% error bounds of the Kolmogorov–Smirnov statistic.*

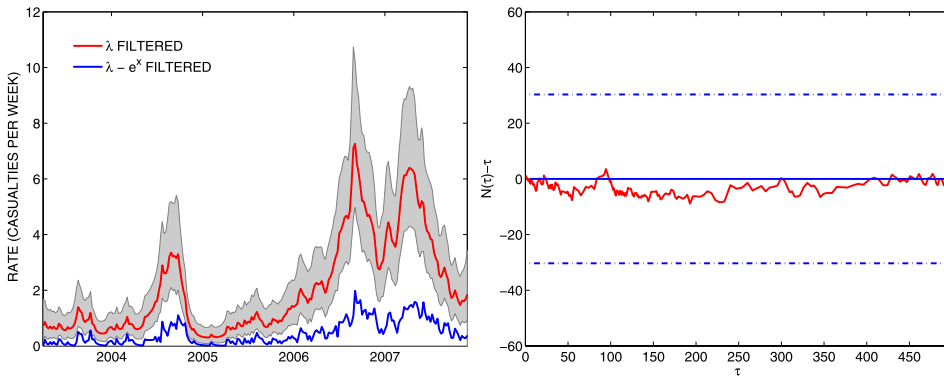


FIG. 10. Civilian casualties in Fallujah. Left: Filtered intensity λ (posterior mean in red, 95% range in grey) and Hawkes rate $\lambda - e^x$ (posterior mean in blue). Right: Normalized cumulative distribution of rescaled event times along with 95% error bounds of the Kolmogorov–Smirnov statistic.

proportion of clustering is attributed to contagion effects, verifying previous work in Lewis et al. (2012). The differences across these three extreme security settings may be due to a variety of factors, such as the security measures employed by the government in power, the organization and tactics of the opposition, the local geography, etc. Trying to determine these underlying factors could be an important line of future research.

5. Discussion. We developed a model and inference methodology to assess the levels of contagion and correlation in crime and security data. We connected Hawkes process and Cox process type models that are typically used independently to explain clustering in crime and security data sets. The high-dimensional nature of the problem, filtering the latent vector \vec{x} , was overcome by using a model with a sparse covariance matrix and a Hawkes component that can be written as a differential equation.

Determining whether contagion effects are present in security related time series is a problem of practical importance. The effectiveness of policing strategies such as *cops on the dots*, where police react to recent crimes [Jones, Brantingham and Chayes (2010)], depends on how the crime event history influences future crime rates. Accurate assessment of the timescale associated with contagion effects may tell police how long they need to put additional patrols in a neighborhood. If exogenous effects are also causing crime rate fluctuations, these effects need to be taken into account if parameter estimates are to be accurate. Similar considerations may be relevant to military strategies in extreme security settings.

For these types of applications, spatial-temporal processes are needed and we believe our methodology should extend to this setting. In Girolami and Calderhead (2011), the authors illustrate the feasibility of Hamiltonian and Langevin Monte Carlo in high-dimensional settings, in particular, for a 2D LGCP. To add time and

self-excitation, several approaches could be used to model the Cox process: choosing a model with sparse inverse covariance matrix, modeling the inverse covariance matrix explicitly, using a sparse approximation, or via a nonparametric sparse estimator, such as l_1 penalization. Spatial extensions will be the focus of subsequent research.

REFERENCES

- BOWERS, K. J., JOHNSON, S. D. and PEASE, K. (2004). Prospective hot-spotting the future of crime mapping? *British Journal of Criminology* **44** 641–658.
- BRIX, A. and DIGGLE, P. J. (2001). Spatiotemporal prediction for log-Gaussian Cox processes. *J. R. Stat. Soc. Ser. B Stat. Methodol.* **63** 823–841. [MR1872069](#)
- CSEKE, B. and HESKES, T. (2011). Approximate marginals in latent Gaussian models. *J. Mach. Learn. Res.* **12** 417–454. [MR2783173](#)
- EGESDAL, M., FATHAUER, C., LOUIE, K. and NEUMAN, J. (2010). Statistical and Stochastic Modeling of Gang Rivalries in Los Angeles. *SIAM Undergraduate Research Online* **3** 72–94.
- GIESECKE, K. and SCHWENKLER, G. (2011). Filtered likelihood for point processes. Available at SSRN 1898344.
- GIROLAMI, M. and CALDERHEAD, B. (2011). Riemann manifold Langevin and Hamiltonian Monte Carlo methods. *J. R. Stat. Soc. Ser. B Stat. Methodol.* **73** 123–214. [MR2814492](#)
- HEGEMANN, R., LEWIS, E. and BERTOZZI, A. (2012). An “Estimate & Score Algorithm” for simultaneous parameter estimation and reconstruction of missing data on social networks. Unpublished manuscript.
- JONES, P. A., BRANTINGHAM, P. J. and CHAYES, L. (2010). Statistical models of criminal behavior: The effects of law enforcement actions. *Mathematical Models and Methods in Applied Sciences* **20** 1397–1423.
- LEWIS, E. and MOHLER, G. (2011). A nonparametric EM algorithm for multiscale Hawkes processes. Unpublished manuscript.
- LEWIS, E., MOHLER, G., BRANTINGHAM, P. J. and BERTOZZI, A. L. (2012). Self-exciting point process models of civilian deaths in Iraq. *Security Journal* **25** 244–264.
- MANGION, A. Z., YUAN, K., KADIRKAMANATHAN, V., NIRANJAN, M. and SANGUINETTI, G. (2011). Online variational inference for state-space models with point-process observations. *Neural Comput.* **23** 1967–1999. [MR2839905](#)
- MARSAN, D. and LENGLINÉ, O. (2008). Extending earthquakes’ reach through cascading. *Science* **319** 1076–1079.
- MOHLER, G. O., SHORT, M. B., BRANTINGHAM, P. J., SCHOENBERG, F. P. and TITA, G. E. (2011). Self-exciting point process modeling of crime. *J. Amer. Statist. Assoc.* **106** 100–108. [MR2816705](#)
- MÖLLER, J. and WAAGEPETERSEN, R. P. (2003). *Statistical Inference and Simulation for Spatial Point Processes* **100**. Chapman & Hall/CRC, Boca Raton, FL. [MR2004226](#)
- OGATA, Y. (1988). Statistical models for earthquake occurrences and residual analysis for point processes. *J. Amer. Statist. Assoc.* **83** 9–27.
- PORTER, M. D. and WHITE, G. (2012). Self-exciting hurdle models for terrorist activity. *Ann. Appl. Stat.* **6** 106–124. [MR2951531](#)
- RUE, H., MARTINO, S. and CHOPIN, N. (2009). Approximate Bayesian inference for latent Gaussian models by using integrated nested Laplace approximations. *J. R. Stat. Soc. Ser. B Stat. Methodol.* **71** 319–392. [MR2649602](#)
- SHAMAN, P. (1969). On the inverse of the covariance matrix of a first order moving average. *Biometrika* **56** 595–600. [MR0255001](#)

- SHORT, M. B., D'ORSOGNA, M. R., BRANTINGHAM, P. J. and TITA, G. E. (2009). Measuring and modeling repeat and near-repeat burglary effects. *Journal of Quantitative Criminology* **25** 325–339.
- SHORT, M., MOHLER, G., BRANTINGHAM, P. and TITA, G. (2010). Gang rivalry dynamics via coupled point process networks. Unpublished manuscript.
- SMITH, A. C. and BROWN, E. N. (2003). Estimating a state-space model from point process observations. *Neural Comput.* **15** 965–991.
- SORNETTE, D. and UTKIN, S. (2009). Limits of declustering methods for disentangling exogenous from endogenous events in time series with foreshocks, main shocks, and aftershocks. *Phys. Rev. E* (3) **79** 061110, 15. [MR2551269](#)
- STOMAKHIN, A., SHORT, M. B. and BERTOZZI, A. L. (2011). Reconstruction of missing data in social networks based on temporal patterns of interactions. *Inverse Problems* **27** 115013, 15. [MR2851919](#)
- TADDY, M. A. (2010). Autoregressive mixture models for dynamic spatial Poisson processes: Application to tracking intensity of violent crime. *J. Amer. Statist. Assoc.* **105** 1403–1417. [MR2796559](#)
- TOWNSLEY, M., JOHNSON, S. D. and RATCLIFFE, J. H. (2008). Space time dynamics of insurgent activity in Iraq. *Security Journal* **21** 139–146.
- VEEN, A. and SCHOENBERG, F. P. (2008). Estimation of space–time branching process models in seismology using an EM-type algorithm. *J. Amer. Statist. Assoc.* **103** 614–624. [MR2523998](#)
- ZAMMIT-MANGION, A., DEWAR, M., KADIRKAMANATHAN, V. and SANGUINETTI, G. (2012). Point process modelling of the Afghan War Diary. *Proc. Natl. Acad. Sci. USA* **109** 12414–12419.

DEPARTMENT OF MATHEMATICS
AND COMPUTER SCIENCE
SANTA CLARA UNIVERSITY
713 HARDING AVE
SAN JOSE, CALIFORNIA 95126
USA
E-MAIL: gmohler@scu.edu